Photocatalytic Scheme with External Magnetic Field on Coffee Waste in Hydrogen Production

Abid Fahreza Alphanoda[1*], Eko Prasetyo[1], and Wisnu Broto[2]

[1]*Department of Mechanical Engineering, Pancasila University, Jl. Lenteng Agung Raya 56 Jakarta Selatan, 12630, DKI Jakarta, Indonesia.*
[2]*Department of Industrial Engineering, Pancasila University, Jl. Lenteng Agung Raya 56 Jakarta Selatan, 12630, DKI Jakarta, Indonesia.*
**Corresponding author: abid_fahreza@univpancasila.ac.id*

Article history:
Received: 27 October 2023 / Received in revised form: 3 November 2023 / Accepted: 17 November 2023
Available online 23 November 2023

ABSTRACT

Photocatalytic is considered a deadlock-breaking technology for renewable energy and lowering environmental pollutants. Photocatalytic efficiency efforts are improved by activating the photocatalyst to introduce an external magnetic field. This review highlights recent breakthroughs by comparing original coffee waste, activation of coffee waste with the addition of catalysts, and manipulation of spin electrons by applying external magnets. Characterization was done with FTIR to look at chemical bonds, UV-Vis with Tauc's Relation approach to measure bandgap, and material morphology using SEM EDX. The increase in photocatalyst activation aligns with the decrease in bandgap value. The rate of decline in bandgap is in line with the rate of acceleration of hydrogen production. Adding an external magnetic increases hydrogen production up to 1.5 times greater than the original photocatalytic.

Keywords: *Bandgap energy, coffee waste, external magnetic field, hydrogen production, photocatalytic, wastewater*

I. Introduction

The main focus of the world today is to develop sustainable transitional energy with priority access in terms of technology and funding [1]. The construction of hydropower, wind, and wave energy plants is an application in supporting renewable energy [2], [3]. However, the need for funds is significant, and it needs research and development of renewable energy that is easily applied and accessed by the community.

Photocatalytic is the process of absorbing photons from solar energy by a photocatalyst to separate H_2O into H_2 and O_2 [4]. Photons can inhibit hole and electron recombination in the photocatalyst to maximize Oxygen Evolution Reaction (OER) and Hydrogen Evolution Reaction (HER) [5]. The efficiency of oxidation and reduction reactions in water can be measured through bandgap energy. The smaller bandgap distance facilitates the release of electrons in the conduction band and reduces hydrogen bonds to break covalent bonds at H_2O [6]. Therefore, it is necessary to present the use of solar energy to be converted into renewable energy, namely hydrogen energy.

Photocatalytic performance is limited by several factors: (1) light absorption, (2) surface redox reactions, and (3) photogeneration separation [7]–[9]. Such factors are reached through doping and defects, surface structure, and charge separation efficiency via

DOI: 10.17977/um016v7i22023p181

heterojunctions [10]. In addition, the addition of an external magnetic field to the water separation process in hydrogen production was successfully created through the electrolysis process. The magnetic field can induce Lorentz to separate anions and cations and adjust the electronic configuration, i.e., the spin orientation of electrons [6]. However, charge separation in electrolysis requires a continuous supply of electrical energy, generally accompanied by complicated devices and high energy purchase costs. Then, it requires material treatment that is easy to apply and inexpensive materials.

The main focus today is the emphasis on recycling household wastewater with hydrothermal processes in the formation of photocatalysts. Coffee waste represents one of the Persistent Organic Pollutants (POPs) in the form of a solution. POPs can be photosensitizers in absorbing UV wavelengths and photocatalysts in producing bandgap [11]. The formation of photocatalysts from waste into carbon, graphite, and graphene structures continues to be carried out today. Hydrothermal is a method that is easy to apply, relatively inexpensive, and uses no complicated tools. In this study, coffee will be activated as a photocatalyst. Measurements of hydrogen production are measured in a photocatalytic process.

II. Material and Methods

1. Material

Materials of Arabica (AR) and Robusta (RB) coffee were obtained from Aceh Gayo plantations in Indonesia. All reagents used commercial materials without further purification and were filtered using a size of 200 mesh. AR and RB were formed with the addition of 350 ml of deionized water and NaOH (75%, supplied by Sigma Aldrich) stratified variations (original, 10 mol, 20 mol, 30 mol, and 40 mol). Each reagent was then centrifuged for 1 hour and then dried at 280°C for 2 hours. All reagents were washed using water and ethanol. The desorption adsorption equilibrium between the reagent and water was set in the dark for 30 minutes.

2. Material Characterization

Optical absorption was tested with UV-Vis reflection spectra in the range of 200 – 800 nm (Specord 200 Plus Analytic Jena UV-Vis Spectrophotometer). The energy band gap (Eg) is obtained through Tauc's Relation approach, as in equation 1.

$$\alpha h\nu = A(h\nu - E_g)^{\frac{n}{2}} \quad \ldots\ldots\ldots\ldots\ldots\ldots\ldots\ldots\ldots\ldots\ldots\ldots\ldots\ldots\ldots\ldots\ldots\ldots\ldots\ldots\ldots\ldots \quad (1)$$

Where α is the absorption coefficient of the semiconductor represented by, hv is the energy of the photon, and A is the constant. The value of n depends on the type of optical transition of the semiconductor (n=1 for direct transition and n=4 for indirect transition) [12], [13].

Determination of functional groups was tested using IRPrestige21, Fourier Transformation Infrared/FTIR (Shimadzu, Japan). Absorbance measurements occur in the infrared radiation range to determine changes in the composition of structures and molecules that occur. Morphological samples of materials and elements using the FEI Inspect S50 testing tool with Energy Dispersive X-ray (EDX). SEM results were analyzed using ImageJ software with accumulated 3D surface plots where data processing was based on dots in each pixel.

3. Photocatalytic Experiments

500 W halogen lamp with calibration of light wavelength measurement was conducted using Aurora 4000 spectrometer (Changchun, China) with spectral range 350 – 1100 nm and light intensity 4000-5600 counts. Visible lighting was done using a focus lens only about the photocatalyst and was controlled at a temperature of 30°C for 7200 seconds. An external fixed magnet was added to the experimental apparatus installation, as shown - in Figure 1.

The MQ-8 sensor, as a hydrogen sensor, has 4 input voltages that are directly related to VCC DC 5V. There is a microtube made of Al_2O_3 with a crossing mechanism between the heater and Au-Pt electrodes and a gas sensing layer made of SnO_2. This electrode and sensing gas are connected to V_{RL}, which will convert and connect on an analog read. The potential difference read in analog read will cause obstacles detected in R_L connected to digital read. The R_L resistance consists of R_S/R_O, where the R_S sensor resistance is at 1000 ppm H_2, and the R_O sensor resistance is in the test. So, the calibration of R_S at 1000 ppm H_2 on the sensor needs to be done to compare with the measurement results.

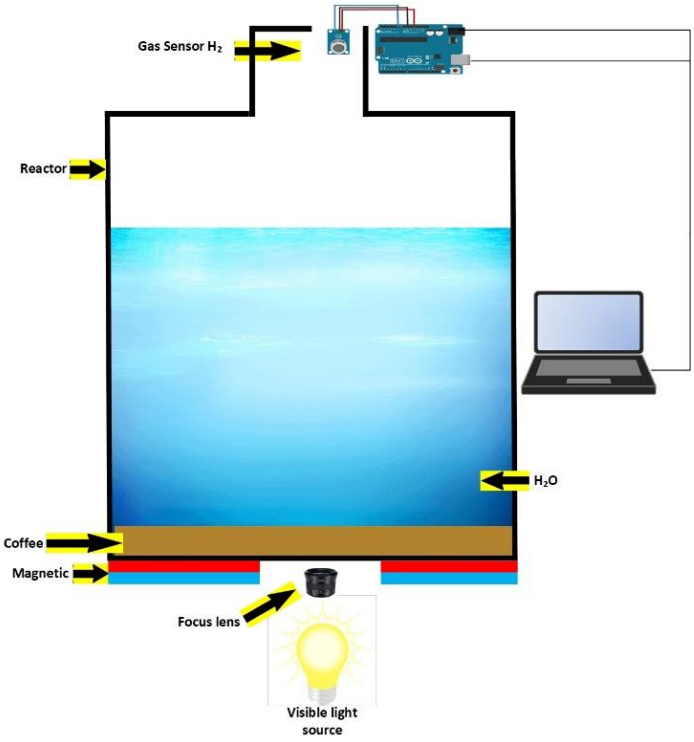

Fig. 1. Experimental apparatus.

III. Results and Discussions

1. Results Characteristics and Morphology of Waste Coffee

FTIR tests bonding characteristics on AR and RB materials, as shown in Figure 2. The absorption at 2900 cm^{-1} is naturally owned by AR and RB, namely alkyl groups. The alkyl group is a CH group owned by aromatic organics clarified by the absorption of C=C-C aromatic ring stretch between 1450-1615 cm^{-1}. After combining with water, AR and RB show OH bonds at 3000 cm^{-1}-3500 cm^{-1} absorption.

The morphological characteristics of AR and RB were analyzed using SEM, as shown in Figure 3. The hydrothermal process in AR and RB shows the structure of natural porosity, as seen in Figure 3(a)(b). Adding NaOH catalyst increases porosity structure, as shown in Figure 3(c)(d). Maximum observation with 3D Surface Plot ImageJ processing is done to see the gradient of positive and negative peaks in the field of view, as seen in Figure 4. It can be seen that AR with hydrothermal structure has less porosity than AR with the addition of NaOH catalyst, respectively, in the image. This happened again with RB with the addition of NaOH catalysts, respectively, in the image. In each AR and RB after the addition of the catalyst, the presence of increased negative peaks indicates the presence of aromatic carbon [6], [14], [15]. This is supported by the EDX results, where the amount of carbon increases after activation of the NaOH catalyst, as shown in Table 1.

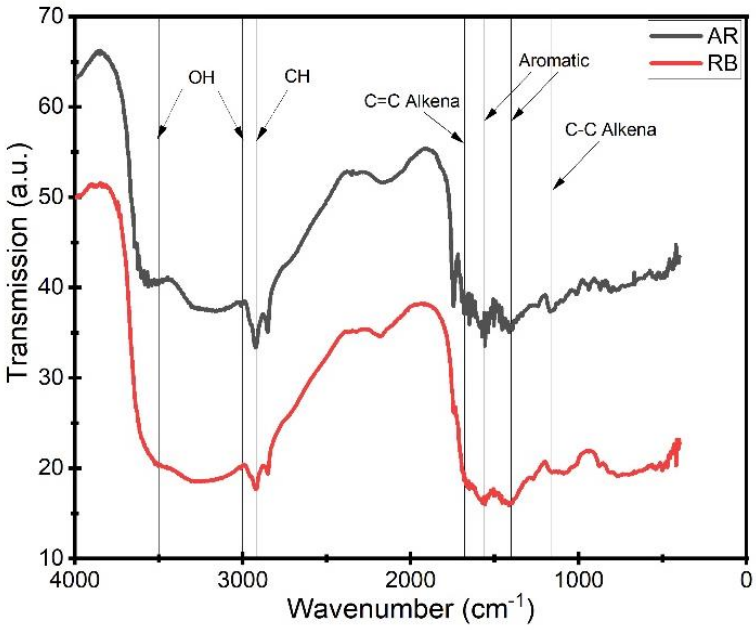

Fig. 2. Comparison of FTIR AR and RB results.

Table 1. EDX Results

EDX Sample	Atomic Percentage (%)		
	C	O	K
AR	68.7	31.0	0.3
RB	68.9	30.8	0.3
AR with catalyst	72.3	27.5	0.2
RB with catalyst	72.8	27.0	0.2

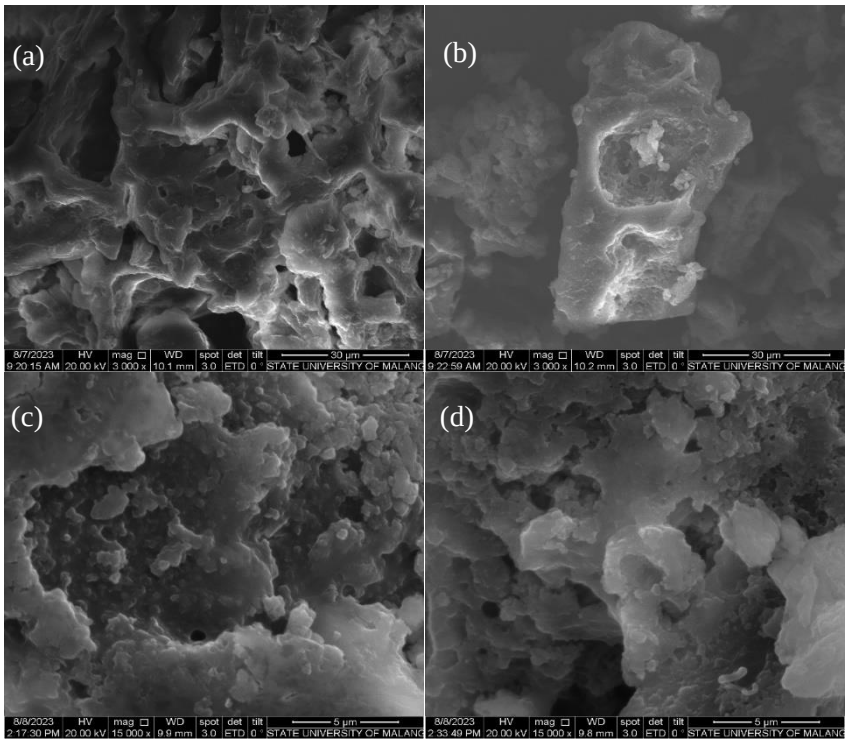

Fig. 3. SEM results (a) AR, (b) RB, (c) AR with NaOH activation, (d) RB with NaOH activation.

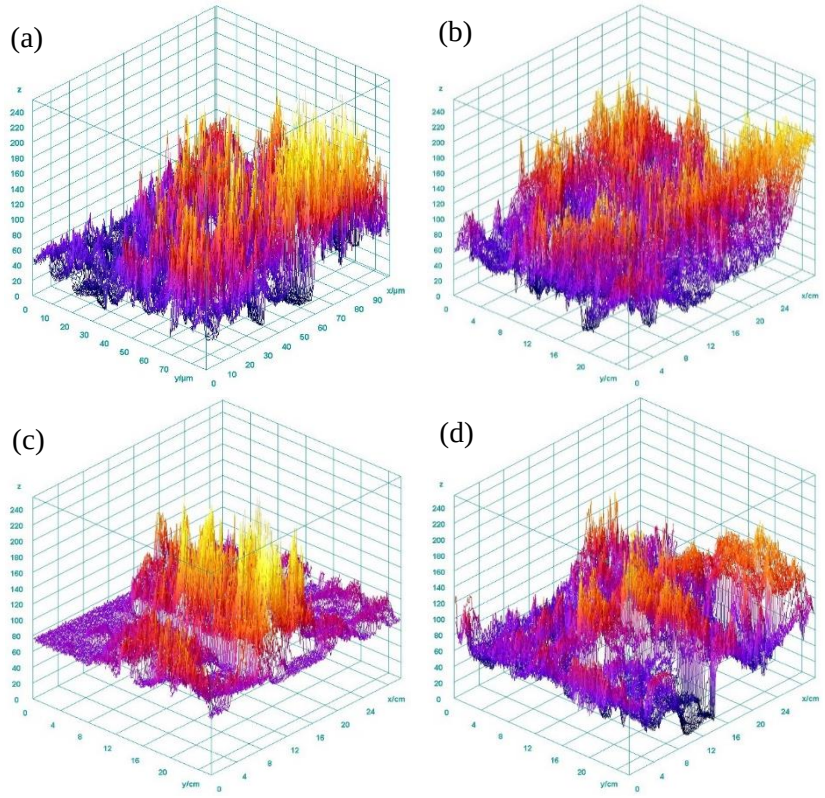

Fig. 4. 3D surface plot with ImageJ (a) AR, (b) RB, (c) AR with NaOH activation, (d) RB with NaOH activation.

2. Results Bandgap Coffee Waste with Catalyst Variation

The determination of bandgap energy was tested based on UV-Vis light absorption and then converted using Tauc's Relation, shown in Figures 5(a) and 5(b). The obtained semiconductor Eg values are seen in Figures 5(c) and 5(d), which have been determined and calculated in Equation (1). From these calculations, bandgap energy in AR and RB varies with catalyst activator treatment indicators, namely original, 10 mol, 20 mol, 30 mol, and 40 mol. The greater the treatment, the molarity value of the catalyst is aligned with the narrowing of the bandgap distance.

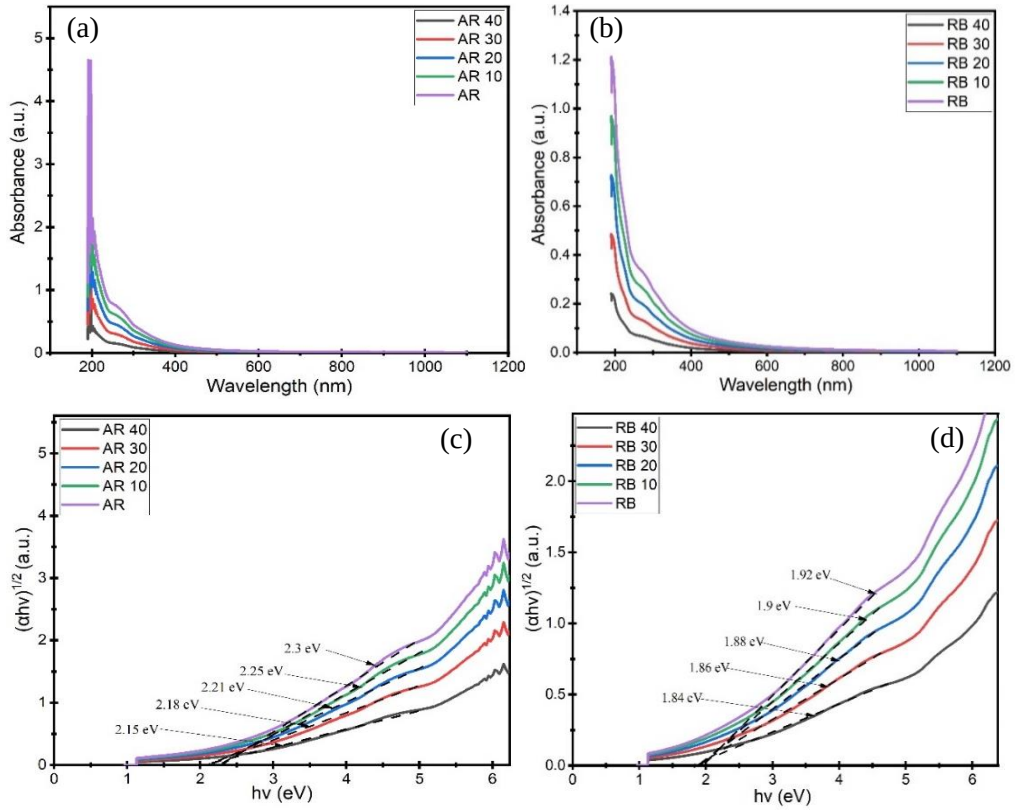

Fig. 5. (a) UV-Vis AR test results, (b) UV-Vis RB test results, (c) Tauc's Relation AR results, (d) Tauc's Relation RB results.

3. Performance of Hydrogen Production with the Addition of External Magnetic Field

Based on the results of Tauc's Relation approach, it was found that the RB bandgap value was smaller than AR. The bandgap values of RB, RB 10, RB 20, RB 30, and RB 40 are 1.92 eV, 1.9 eV, 1.88 eV, 1.86 eV, and 1.84 eV respectively. AR, AR 10, AR 20, AR 30, and AR 40 bandgap values are 2.3 eV, 2.25 eV, 2.21 eV, 2.18 eV, and 2.15 eV, respectively. Increasing the activation treatment of the amount of molarity NaOH can increase the acceleration rate of hydrogen production. High rates affect the efficiency of hydrogen production time but do not affect the amount of hydrogen produced. The hydrogen production rate in AR is seen in Figure 6(a), while the hydrogen production rate in RB is seen in Figure 6(b). Photocatalyst irradiation can produce holes and electron pairs due to photons adsorbed on the surface. Holes are created by electron jumps from the valence band (VB) to the conduction band (CB). Holes will cause an oxidation process in water to turn

into hydroxyl. At the same time, the electron jump in the valence band will reduce water to produce hydron. This hydron is the forerunner of hydrogen gas. Rapid recombination of photocatalysts reduces the efficiency of oxidation-reduction reactions. One result is the small amount of hydrogen formed. The addition of external magnets is the most hotly discussed issue. External magnetism is a magnetic field where the amount of charge, speed, and strength of the magnet determines the Lorentz Force. In photocatalytics, holes and electrons are excited by photons. When holes and electrons move because they are affected by the external magnetic field, they will undergo opposite forces. As a result, the recombination of holes and electrons will be inhibited. This is evidenced by increased hydrogen AR and RB production when the photocatalytic process is coupled with external magnets. As shown in Figures 6(c) and 6(d), the increase in hydrogen production for AR and RB is almost 1.5 times compared to the original photocatalytic.

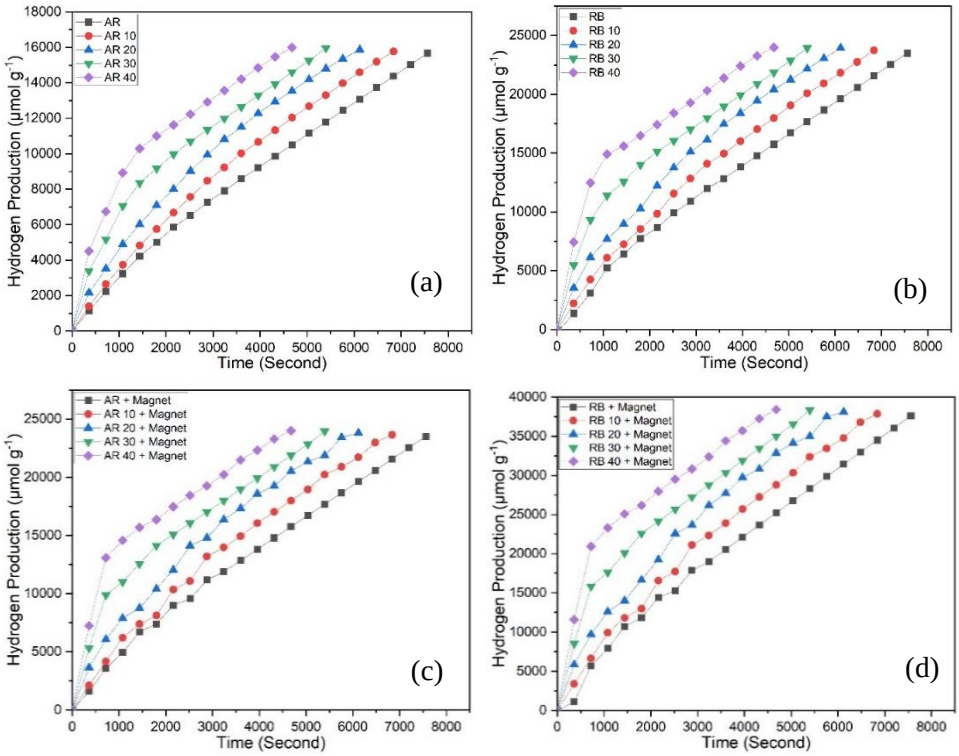

Fig. 6. (a) Production of hydrogen AR, (b) Production of hydrogen RB, (c) Production of hydrogen AR + Magnet, (d) Production of hydrogen RB + Magnet.

IV. Conclusions

The formation of photocatalysts from coffee waste was successfully carried out by hydrothermal method. Activation of photocatalysts using NaOH affects the bandgap value. Increased molarity tends to result in a smaller bandgap of coffee waste. This can be seen by the emergence of aromatic organics in the form of porosity, and the value of the amount of carbon increases. The bandgap reduction rate can be in line with the rate of acceleration of hydrogen production, where time is getting shorter. However, this does not affect the amount of hydrogen produced. The production of hydrogen with the addition of external magnets affects up to 1.5 times greater than the original photocatalytic.

Acknowledgment

This study was provided by the Faculty of Engineering, University of Pancasila, in the 2023 Middle Research Grant Program. The authors would like to thank the Advanced Minerals and Materials Laboratory, Universitas Negeri Malang, and Pancasila University Laboratory.

References

[1] T. Uekert, C. M. Pichler, T. Schubert, and E. Reisner, 'Solar-driven reforming of solid waste for a sustainable future', *Nat Sustain*, vol. 4, no. 5, pp. 383–391, May 2021, doi: 10.1038/s41893-020-00650-x.

[2] M. Mariello, F. Guido, V. M. Mastronardi, M. T. Todaro, D. Desmaële, and M. De Vittorio, 'Nanogenerators for harvesting mechanical energy conveyed by liquids', *Nano Energy*, vol. 57, pp. 141–156, 2019, doi: 10.1016/j.nanoen.2018.12.027.

[3] J. Kotowicz, Ł. Bartela, D. Węcel, and K. Dubiel, 'Hydrogen generator characteristics for storage of renewably-generated energy', *Energy*, vol. 118, pp. 156–171, 2017, doi: 10.1016/j.energy.2016.11.148.

[4] Y. He, K. Chen, M. K. H. Leung, Y. Zhang, L. Li, G. Li, J. Xuan, and J. Li, 'Photocatalytic fuel cell – A review', *Chemical Engineering Journal*, vol. 428, no. July 2021, 2022, doi: 10.1016/j.cej.2021.131074.

[5] L. Clarizia, M. N. Nadagouda, and D. D. Dionysiou, 'Recent advances and challenges of photoelectrochemical cells for hydrogen production', *Curr Opin Green Sustain Chem*, vol. 41, Jun. 2023, doi: 10.1016/j.cogsc.2023.100825.

[6] Purnami, N. Hamidi, M. N. Sasongko, D. Widhiyanuriyawan, and I. N. G. Wardana, 'Strengthening external magnetic fields with activated carbon graphene for increasing hydrogen production in water electrolysis', *Int J Hydrogen Energy*, vol. 45, no. 38, pp. 19370–19380, 2020, doi: 10.1016/j.ijhydene.2020.05.148.

[7] S. Balachandran and M. Swaminathan, 'The simple, template free synthesis of a Bi2S3-ZnO heterostructure and its superior photocatalytic activity under UV-A light', *Dalton Transactions*, vol. 42, no. 15, pp. 5338–5347, 2013, doi: 10.1039/c3dt33117b.

[8] T. Li, M. Ruan, Z. Guo, C. Wang, and Z. Liu, 'Modulation of Lewis and Brønsted Acidic Sites to Enhance the Redox Ability of Nb2O5 Photoanodes for Efficient Photoelectrochemical Performance', *ACS Appl Mater Interfaces*, vol. 15, no. 9, pp. 11914–11926, Mar. 2023, doi: 10.1021/ACSAMI.2C23284/SUPPL_FILE/AM2C23284_SI_001.PDF.

[9] S. Liu, Y. Hu, Y. Huang, W. Wang, P. Deng, L. Zhang, W. Xuan, and Y. Hou, "A 'battery' like Z-scheme heterojunction photocatalyst fabricated from aminated CdS and Ni3-polyoxometalate for promoted hydrogen production and electron transfer mechanism studies," *Int J Hydrogen Energy*, 2023, doi: https://doi.org/10.1016/j.ijhydene.2023.07.154.

[10] Z. Xie, G. Liu, L. Xie, P. Wu, H. Liu, J. Wang, Y. Xie, J. Chen, and C.-Z. Lu, "Promoting photocatalytic H2 evolution through interfacial charge separation on the direct Z-scheme ZnIn2S4/ZrO2 heterojunction," *Int J Hydrogen Energy*, vol. 48, no. 84, pp. 32782–32796, 2023, doi: https://doi.org/10.1016/j.ijhydene.2023.05.038.

[11] Z. Liu, X. Sun, J. Fu, W. Liu, and Z. Cai, 'Elevated nitrate promoted photodegradation of PAHs in aqueous phase: Implications for the increased nutrient discharge', *J Hazard Mater*, vol. 443, Feb. 2023, doi: 10.1016/j.jhazmat.2022.130143.

[12] P. R. Jubu, O. S. Obaseki, A. Nathan-Abutu, F. K. Yam, Y. Yusof, and M. B. Ochang, 'Dispensability of the conventional Tauc's plot for accurate bandgap determination from UV–vis optical diffuse reflectance data', *Results in Optics*, vol. 9, Dec. 2022, doi: 10.1016/j.rio.2022.100273.

[13] A. Bhogi, B. Srinivas, M. Shareefuddin, and P. Kistaiah, 'Band gap determination by Tauc's, ASF and DASF methods of alkaline earth modified lithium borate glasses co-doped with transition metal ions', *Mater Today Proc*, 2023, doi: 10.1016/j.matpr.2023.04.243.

[14] P. Purnami and Y. Komaril, 'The enhancement of magnetic field assisted water electrolysis hydrogen production from the compact disc recordable waste polycarbonate layer', *Int J Hydrogen Energy*, vol. 48, no. 48, pp. 18154–18165, 2023, doi: https://doi.org/10.1016/j.ijhydene.2023.01.329..

[15] N. W. Satrio, Winarto, Sugiono, and I. N. G. Wardana, 'Hydrogen production from instant noodle wastewater by organic electrocatalyst coated on PVC surface', *Int J Hydrogen Energy*, vol. 45, no. 23, pp. 12859–12873, 2020, doi: 10.1016/j.ijhydene.2020.03.002.